Published in final edited form as:
J Appl Physiol. 2005 September ; 99(3): 1138–1148. doi:10.1152/japplphysiol.00668.2004.

Computational simulation of human upper airway collapse using a pressure-/state-dependent model of genioglossal muscle contraction under laminar flow conditions

Yaqi Huang, **Atul Malhotra**, and **David P. White**
Department of Medicine, Division of Sleep Medicine, Brigham and Women's Hospital and Harvard Medical School, Boston, Massachusetts

Abstract

A three-element, pressure- and state (sleep and wake) -dependent contraction model of the genioglossal muscle was developed based on the microstructure of skeletal muscle and the cross-bridge theory. This model establishes a direct connection between the contractile forces generated in muscle fibers and the measured electromyogram signals during various upper airway conditions. This effectively avoids the difficulty of determining muscle shortening velocity during complex pharyngeal conditions when modeling the muscle's contractile behaviors. The activation of the genioglossal muscle under different conditions was then simulated. A sensitivity analysis was performed to determine the effects of varying each modeled parameter on the muscle's contractile behaviors. This muscle contraction model was then incorporated into our anatomically correct, two-dimensional computational model of the pharyngeal airway to perform a finite-element analysis of air flow, tissue deformation, and airway collapse. The model-predicted muscle deformations are consistent with previous observations regarding upper airway behavior in normal subjects.

Keywords

genioglossus; muscle activity; finite element; pharyngeal airway; collapsibility

The rationale for developing a genioglossal muscle contraction model comes from the study of obstructive sleep apnea, a common disorder characterized by repetitive collapse of the pharyngeal airway during sleep (40, 61). This results in sleep disruption, hypersomnolence, and decreased quality of life in addition to potential adverse cardiovascular outcomes (24, 28, 29, 48, 51). However, understanding the pathophysiology of this disorder is hampered primarily by the complexity of the pharyngeal airway. Due to the limits of human experimentation and lack of suitable animal models, our knowledge of pharyngeal physiology has remained limited. We believe a sophisticated computational model of the human upper airway could overcome the limitations of experimental studies and help guide future investigations of the pathophysiology of sleep apnea, as well as potentially the treatment options for this common disorder.

One of the major difficulties in developing such a computational model is the simulation of contractile behaviors of pharyngeal muscles, especially the genioglossal muscle, under different experimental conditions. Substantial evidence in animals and humans has shown

Address for reprint requests and other correspondence: Y. Huang, Sleep Disorders Program @ BI, Brigham and Women's Hospital, 75 Francis St., Boston, MA 02115 (yhuang@rics.bwh.harvard.edu).

that the activity of the upper airway dilator muscles plays an important role in maintaining airway patency during breathing (42, 43, 58). Studies of the control of genioglossal muscle activity, both awake and asleep, strongly indicate that the principal stimulus to inspiratory activity of this muscle is negative intrapharyngeal pressure, although phasic respiratory input is active as well (3, 18, 20, 38, 42, 43, 55). During sleep, upper airway muscles respond less to negative intrapharyngeal pressure, yielding a vulnerable airway that cannot adequately respond to threats to its patency (19, 42). Thus the airway is more collapsible asleep (39).

We have recently developed a two-dimensional finite-element model of the pharyngeal airway to investigate the influence of the anatomic variability (particularly in upper airway length) between men and women on upper airway collapsibility (22, 37). In that model, we accounted for the effects of tongue muscle activation during sleep by simply changing the tissue elastic modulus instead of developing a direct simulation of muscle contraction. It is apparent, however, that if we want to develop a more complex and accurate simulation of upper airway behavior, particularly if we want to investigate the effects of muscle contraction on upper airway collapsibility, a more realistic tongue muscle (genioglossal muscle) activation model is needed. Currently, there are models of the tongue describing its movements during mastication, swallowing, and speech (17, 46, 49). However, none of these models mimics genioglossal activation during the development of negative airway pressure as occurs during respiration. In addition, the existing contractile models for skeletal muscle generally require the shortening velocities of muscle fibers as the model input when calculating the contractile force (14, 30, 33), which are difficult if not impossible to determine for the genioglossal muscle under complex pharyngeal conditions. A common way to evaluate the activation of a pharyngeal muscle in clinical studies is to measure its electromyogram (EMG) under a variety of conditions. A larger EMG value represents a higher level of muscle activation and therefore a larger contractile force. We believe that a proper model can establish a direct connection between the contractile force and the measured EMG signal. If a mathematical relationship between the EMG signal and the contractile force can be established, this contraction model would be more convenient and more applicable than one requiring fiber-shortening velocities in upper airway computational simulations.

In the present study, we focused on developing, based on the microstructure of skeletal muscle and the cross-bridge theory (25, 26, 44), a three-element, pressure- and state (sleep and wake)-dependent contraction model of the genioglossal muscle, which establishes a direct connection between the contractile forces generated in muscle fibers and the measured EMG signals during various upper airway conditions. Thus the activation of the genioglossal muscle under different conditions is simulated. A sensitivity analysis was then performed to determine the effects of varying each modeled parameter on the muscle's contractile behaviors. We also incorporated this muscle contraction model into our anatomically correct, two-dimensional computational model of the pharyngeal airway to mimic air flow, tissue deformation, and airway collapse. However, it needs to be clearly stated that, in addition to the genioglossal muscle, other upper airway dilator muscles, as well as pharyngeal constrictor muscles, are active awake and asleep and, therefore, contribute to upper airway patency (12, 35, 41). In a complete clinical simulation of upper airway collapse, the effects of these muscles on upper airway collapsibility must be considered. In the present study, incorporating only the genioglossus model into our computational simulation of pharyngeal behaviors does not mean that the effects of other muscles are not important. It only serves our purpose, which is to test this genioglossal muscle contraction model and to determine how the activity of this muscle can affect upper airway patency during breathing. The development and testing of such a muscle contraction model is a key step in developing a complete three-dimensional upper airway computational model, which

could potentially, in the future, play an important role in surgical planning or other therapeutic approaches.

METHODS

Pressure- and state-dependent muscle contraction model

In this model, airway negative pressure is the main stimulus to muscle activation. However, the effects of state (awake or asleep) are also included. Both expiratory tonic and inspiratory phasic activation of the genioglossal muscle along its fiber's axial direction are also simulated. This genioglossal muscle contraction model is constructed based on the microstructure of skeletal muscle.

Like the well-known Hill's three-element model of skeletal muscle (14), this genioglossal muscle model includes a parallel element, a series element, and a contractile element (see Fig. 1). We describe the parallel element, which mainly represents connective tissue, as a linear elastic material in which stress is linearly related to strain

$$\sigma_p = C\varepsilon_p \quad (1)$$

where, for a one-dimensional muscle fiber model, C is simply the Young's modulus E, and σ_p and ε_p are the stress and strain of the parallel element along the fiber's orientation, respectively. For a two-or three-dimensional muscle model, C, consisting of Young's modulus E and Poission ratio ν, is the elastic constitutive matrix, and σ_p and ε_p are the stress and strain tensors in the parallel element, respectively.

The series element, which comes mainly from the myosin and actin filaments, is modeled as a nonlinear elastic material

$$\sigma_{szz} = \beta(e^{\alpha\varepsilon_{szz}} - 1) \quad (2)$$

where σ_{szz} and ε_{szz} are the normal stress and strain in the fiber's axial direction in the series element, respectively, with α and β being constants and e begin the base of the natural logarithm.

The contractile element is the active part in generating a rapid shortening along the fiber's axial direction, which is controlled by the central neuron. The modeling of contraction is based on the cross-bridge theory (44), which proposes that the generation of force is due to the attachment of the cross bridges to the actin filament. In our model, the number of attached cross bridges is described as a function of both the negative upper airway pressure and the physiological state (passive, asleep, or awake). When the upper airway pressure changes, feedback is sent to the mechanoreceptor and the level of muscle activity is adjusted. We assume that, in the passive condition, all cross bridges are detached and that the actin and myosin can freely slide. Therefore, in the passive airway, only the parallel element contributes to the fiber's elasticity. In the waking condition, the number of the attached cross bridges will continuously increase with a decrease in upper airway pressure, thereby maintaining upper airway patency. During sleep, the number of attached cross bridges and, therefore, the contraction increase very slowly with a decrease in airway pressure due to a substantial reduction but not complete loss of reflex mechanisms (10, 52). The contractile element is modeled by

$$\sigma_{szz}=kN\left[\frac{2y_0}{L_{sar}}+\varepsilon_{czz}\right] \quad (3)$$

where k is th spring coefficient for a single bridge, N is the number of attached cross bridges, y_0 is required displacement for generating the initial contractile force, L_{sar} is the length of a sarcomere, and ε_{czz} is the strain of cross bridges in the fiber's axial direction during contraction. A large EMG amplitude (A_{EMG}) is interpreted as a large number of attached cross bridges, which can generate a large contractile force. Our goal is to establish a mathematical relationship between the EMG and the number of cross bridges so that we can directly use experimental information to calculate the contractile force. We thus avoid using contraction velocity in various complex pharyngeal conditions, which cannot be accurately determined. As seen in Eq. 2, the series element elongates nonlinearly with a linear increase in contractile force. If the overall muscle fiber length is largely maintained during the waking condition, the contractile element should shorten nonlinearly with the contractile force, which basically requires a nonlinear relationship between N and A_{EMG}. We have tested different mathematical relationships between N and A_{EMG} to assess their effects on the total fiber length under different outside loads. Based on our numerical testing results, we chose a nonlinear relationship between N and the measured A_{EMG}, and therefore a nonlinear relationship between N and the epiglottis negative pressure P

$$N=a[A_{EMG}(P)]^m \quad (4)$$

where a and m (>1) are constants, and (P) indicates that A_{EMG} is a function of P (pressure). Therefore, Eq. 3 can be rewritten as

$$\sigma_{szz}=c\,A_{EMG}^m\left(\frac{2y_0}{L_{sar}}+\varepsilon_{czz}\right) \quad (5)$$

where $c = ka$. This gives the relationship between the contractile stress in the fiber's axial direction and A_{EMG}.

The total normal stress in the fiber's axial direction (σ_{zz}) is

$$\sigma_{zz}=\sigma_{pzz}+\sigma_{szz} \quad (6)$$

where σ_{pzz} is the normal stress in the parallel element. The total strain in the fiber's axial direction ε_{zz}, which is equal to the strain in the parallel element ε_{pzz}, is the sum of the strain in the series element ε_{szz} and the strain in the contractile element ε_{czz}:

$$\varepsilon_{zz}=\varepsilon_{pzz}=\varepsilon_{szz}+\varepsilon_{czz} \quad (7)$$

From Eqs. 2, 5, and 7, one can obtain the relationship between the contractile stress σ_{szz} and the total normal strain ε_{zz} in the fiber's axial direction

$$\varepsilon_{zz}=\frac{1}{\alpha}\ln\left(\frac{\sigma_{szz}}{\beta}+1\right)+\frac{\sigma_{szz}}{c\,A_{EMG}^m}-\frac{2y_0}{L_{sar}} \quad (8)$$

Equations 1, 6, and 8 give the constitutive relationship in the fiber's axial direction. In the perpendicular direction, we use linear elastic constitutive equations. This contraction model will be incorporated into the overall computational model of the pharyngeal airway when undertaking our airway collapse analysis.

Parameter determination

The determination of the y_0, c, and m is based on measured data in the waking upper airway. The parameter y_0 can be estimated by the muscle fiber shortening in a specific genioglossal condition: when the contractile stress σ_{szz} is zero, we have, from Eq. 5, the normal strain in the contractile element

$$\varepsilon_{czz}=-\frac{2y_0}{L_{sar}} \quad (9)$$

and, from Eq. 2, the normal strain in the series element ε_{szz} is zero. Therefore, the total strain in the parallel element is

$$\varepsilon_{zz}=\varepsilon_{czz}=-\frac{2y_0}{L_{sar}} \quad (10)$$

This minimal contractile force state should correspond to the minimal number of the attached cross bridges, which is achieved when A_{EMG} reaches its lowest value in tonic activation during expiration. If we know the total normal stress loaded on the muscle fiber at this moment to be σ_0, after substituting $\sigma_p = \sigma_0$, $C = E$ and $\varepsilon_p = \varepsilon_{zz}$ into Eq. 1, the result is

$$y_0=-\frac{\sigma_0 L_{sar}}{2E} \quad (11)$$

The parameter c can be obtained by substituting Eq. 6 into Eq. 8 with specific stress condition $\sigma_{zz} = 0$ (zero upper airway pressure), which gives

$$c=\frac{-E\varepsilon_{zz0}}{A_{EMG0}^{m}\left[\frac{2y_0}{L_{sar}}+\varepsilon_{zz0}-\frac{1}{\alpha}\ln\left(\frac{-E\varepsilon_{zz0}}{\beta}+1\right)\right]} \quad (12)$$

where A_{EMG0} is the EMG value at zero upper airway pressure, and ε_{zz0} is the corresponding muscle strain under this condition.

The fact that the patency of a normal human upper airway is maintained when P decreases during waking is used to determine m. We can consider that, for a wide range of negative airway pressures, the displacement, and therefore the strain, along the fiber's axial direction is almost constant. Given a group of m values, we calculate c for each m value using Eq. 12 and plot the curve of ε_{szz} vs. σ_{szz} using Eq. 8. Comparing these curves with different values of m, we can find the m value that maintains the fiber's displacement in a large negative pressure range.

The values of y_0, c, and m determined under the waking condition will be used in both the waking and sleeping conditions. However, the function $A_{EMG}(P)$ in the above equations is different between waking and sleeping. During sleep, both tonic and phasic genioglossal muscle activities generally decrease by ~10–20% during normal breathing, which has been observed in many of our laboratory's experimental studies (11, 59). Most of the remaining

tonic and phasic activities represent fundamentally pressure-independent (respiratory) inputs controlled by the central neuron, although we have still programmed it, for convenience, as a function of pressure but not phase or time. At this time, during sleep, the phasic activation increases slowly when upper airway pressure becomes more negative due to a substantial reduction but not complete loss of reflex mechanisms. In an actual simulation of upper airway behavior during sleep using the above muscle contraction model, a measured A_{EMG} curve during sleep is required as an input.

Finally, it should be pointed out that there is a preactivation in the genioglossal muscle before the development of negative airway pressure. Because the measured EMG-pressure curve is used to calculate the number of cross bridges, this preactivation reflected in the EMG signal is also included in our muscle contraction model.

Construction of the geometrical structure of the pharyngeal airway

A two-dimensional geometrical structure of the pharyngeal airway is constructed based on our midsagittal plane magnetic resonance images from normal subjects (see Fig. 2). We define key points along the boundaries of all structures deemed important (tongue, mandible, hard palate, soft palate, uvula, hyoid bone, epiglottis, etc.). The key points are chosen such that each must be crucial in determining geometrical structure and are consistently available on obtained images. A “mean structure” for a specific group of subjects such as men or women can be obtained by averaging the corresponding signals collected from each image. Figure 3 shows a mean structure of the male upper airway obtained from five randomly selected magnetic resonance images of normal men.

Air flow and tissue deformation

The human pharyngeal airway is considered a mechanical system composed of multiple materials and having complex geometric structures. As our laboratory did previously (22, 37), the upper airway is described as a two-dimensional channel in the midsagittal plane. Although this ignores the effects of the lateral walls, this model can mimic the anatomical structure in the midsagittal plane, thereby maintaining the major features of tongue and uvula movement, which play an important role in negative pressure-induced upper airway collapse.

Several basic approximations are used for air flow. Because the pressure drop across the upper airway is small and the flow velocity is generally much smaller than sound speed, we can assume air to be incompressible. We use a laminar flow model to describe the flow in the upper airway. As boundary conditions, the pressures at the entrance and the exit to the upper airway are given. Because the posterior pharyngeal wall is thin and attached to the vertebral bodies, we modeled it as a rigid structure.

For the solid part, the deformation of a tissue is controlled by the geometric equation, equilibrium equation, and constitutive equations given by Eqs. 1, 6, and 8 for the genioglossal muscle, or given simply by a linear equation for all other pharyngeal tissues or bones by assuming that they are linear elastic materials. All soft tissues are assumed to be essentially incompressible. Therefore, each tissue can change its geometric shape under loads but maintains its total area during the deformation for a two-dimensional tissue model or maintains its total volume during the deformation for a three-dimensional tissue model.

In the three-dimensional structure of the upper airway, the soft palate gets support from other muscles such as palatoglossus or palatopharyngeus in the lateral direction. However, when the upper airway is simplified to a two-dimensional channel, these lateral supports are missing. The soft palate and uvula, therefore, become more deformable with this simplification. To compensate for the effect of losing lateral support, we introduce a

"moving together" assumption: we let the soft palate and uvula basically move together with the tongue during negative airway pressure development by adjusting the elastic modulus of the soft palate and uvula to a somewhat higher value. See DISCUSSION for more explanations on this approximation.

The hard palate, mandible, and bottom of the epiglottis are considered fixed boundaries with zero displacement. At the interface of two solid tissues, such as the tongue and hyoid bone, the displacement must be continuous. The anterior part of the tongue and the boundary linking the bottom of the mandible and the bottom of epiglottis are considered free boundaries. The tongue, uvula, and other soft tissue, except the parts connecting directly to fixed boundaries, can move freely under loads. Fluid-solid interaction conditions are used at the deformable front wall of the upper airway, which is composed of the air-uvula, air-tongue, and air-epiglottis interfaces. The solid model calculates the displacement and gives the kinetic condition for the fluid model, and the force distribution calculated from the fluid model gives a dynamic boundary condition for the solid part.

Finite element analysis

The governing equations for air flow and tissue deformation are solved numerically using the finite element method, which is a widely accepted numerical procedure for obtaining solutions to many of the problems encountered in engineering analyses (6). Because the genioglossal muscle only contracts along its fiber's axial direction, we mesh the tongue based on muscle fiber orientation. The constitutive matrix in each element of the genioglossal muscle is first given in the local coordinate system related to fiber orientations, and then it is converted to the global coordinate system for performing the finite element analysis. A nonlinear dynamic analysis software, ADINA (ADINA R & D, Watertown, MA), together with our own software, is used to make this simulation of air flow, tissue deformation, and airway collapse. Eight-node rectangular solid elements and three-node triangular fluid elements are employed.

Model inputs

The mechanical parameters for the genioglossal muscle (E, ν, L_{sar}, α, and β), hard palate, hyoid bone, epiglottis, and air are given in Table 1. Other inputs include epiglottis pressure P and the genioglossal A_{EMG} [$A_{EMG}(P)$] during waking and sleeping; a 0.8-cmH_2O epiglottis pressure corresponding to the EMG value of tonic activity during expiration, which is used to calculate y_0; and a 0.65% muscle shortening at zero epiglottis pressure, which is used to estimate c. Also, a value of 2.3 for the parameter m, which is determined by the procedure described in *Parameter determination*, is used in this simulation.

RESULTS

Muscle fiber stretch

EMG data used to test the contraction model are obtained from published results for the waking condition (3). For the sleeping airway, because no such measured EMG data are available for the same subjects, we estimated that both tonic and phasic genioglossal muscle activities decrease by ~15% during normal breathing based on the literature, and that phasic activation increases slowly when upper airway pressure becomes more negative due to a substantial reduction but not complete loss of reflex mechanisms (see Fig. 4) (10). Figure 5 shows the stretch of the genioglossal muscle fiber during different upper airway pressures and states (passive, sleep, and wake), which is normalized by the stretch of the passive muscle fiber at −5 cmH_2O. From previous studies, we know for the normal male upper airway, that −5 cmH_2O is the average closing pressure (P_{close}) under passive conditions and −13 cmH_2O the average P_{close} under sleeping conditions (27, 50). One can see from this

figure that the genioglossal muscle fiber has a relatively similar stretch at −13 cmH_2O pressure during sleep to that at −5 cmH_2O under the passive condition. For the waking airway, the muscle fiber initial contraction is 38% larger than that in the sleeping airway at zero pressure (muscle preactivation) and then reaches a constant length, which keeps the upper airway open. These results are consistent with the observations of the upper airway under different conditions in normal subjects.

Sensitivity analysis

A sensitivity analysis allows us to ascertain which of the parameters in the muscle contraction model have a significant effect on the muscle contraction behaviors. Table 2 shows the results obtained by varying each parameter by ±30% from its reference value on the change in muscle fiber length (ΔL). All the calculated changes in the muscle fiber length under different pressures and states are normalized by the stretch of the sleeping muscle fiber at −13 cmH_2O pressure (ΔL_0), which is calculated based on reference parameter values. Table 2 includes the results for several representative pressure values. A value of −2 cmH_2O is roughly the peak negative pressure during a normal inspiration while awake, −4 cmH_2O represents the peak negative pressure during inspiration while asleep, and −13 cmH_2O is the mean P_{close} of the male upper airway under the sleeping condition. A positive value in Table 2 represents a stretch, and a negative value represents a shortening in the muscle fiber. One can see from the table that A_{EMG}, the coefficient c in Eq. 5, which is the product of the spring coefficient for a single cross bridge and a parameter relating to the increasing rate of the number of cross bridges, and especially the parameter m in Eq. 4, which gives the nonlinear degree of the relationship between the total number of cross bridges and the A_{EMG}, have a substantial effect on muscle fiber length. In contrast, the changes of α and β in Eq. 2, which characterize the nonlinear elastic deformation of myosin and actin filaments under contractile forces, have only minor effects on muscle stretch.

Two-dimensional simulation of genioglossal muscle contraction

Figure 6 shows simulations of the genioglossal muscle under different conditions. In this figure, each large rectangle represents the genioglossal muscle with a vertical fiber orientation. The upper-left corner of each muscle is fixed. The remainder of the upper boundary can only move horizontally, and the lower boundary is fully free. We simulate genioglossal muscle behavior under four different conditions. Figure 6*A* shows muscle shortening with the increase of the contractile stress without any outside load. In Fig. 6, *B*–*D*, negative pressure is loaded on the lower boundary of the muscle. In Fig. 6*B*, the passive model, there is a maximum stretch at −5 cmH_2O, since this is the P_{close} of the male passive upper airway. Figure 6*C*, the sleeping model, shows that the maximum stretch is at about −13 cmH_2O, which is the P_{close} for the male airway during non-rapid eye movement sleep. Figure 6*D*, the waking model, shows little muscle deformation under a large load due to the strong muscle activation during waking. In addition, from these two-dimensional simulations, one can also see that when an incompressible muscle stretches or contracts in its fiber's axial direction, it will also change its dimension in the perpendicular direction to maintain its original area. These results in Fig. 6 are consistent with the general contractile behaviors of skeletal muscle and the muscular hydrostat theory of tongue function (31, 54).

Flow and deformation

After incorporating the genioglossal muscle contraction model into the two-dimensional finite element upper airway model, we analyze detailed flow, pressure distributions, tongue movement and upper airway collapse. Figure 7 shows tongue deformation and movement in the sleeping condition with various airway negative pressures. In contrast to the results in Figs. 5 and 6, which can only show the effect of the negative pressure-induced genioglossus stretch on pharyngeal collapse, the simulated changes in upper airway size under negative

pressures in Fig. 7 include both the displacement of pharyngeal tissues from the transmural pressure exerted on these tissues and the genioglossal muscle stretch in the fiber's axial direction with a corresponding dimensional change in the perpendicular direction. The dashed lines give the initial locations of the tongue and uvula at zero pressure, and the solid lines show their positions at the given airway negative pressures. Vectors are used to describe the local flow velocities in the upper airway. The arrow for each vector indicates the flow direction and the length, and color represents the magnitude of the velocity. One can see that the flow becomes more complex with a gradual decrease in the upper airway pressure. This is consistent with the observed flow behaviors in the human upper airway and Shome et al.'s simulations (53). In another simulation with the use of a slightly larger contraction than that for Fig. 7, the results indicate that when the upper airway pressure decreases to about −8 cmH_2O, the uvula and posterior portion of the tongue begin to vibrate (animation files are available on CD). This vibration results from the strong interaction between the complex flow and the collapsible pharyngeal wall when the upper airway becomes narrow and the flow velocity is high at substantial negative pressures. The frequency of this vibration depends on how fast the upper airway pressure decreases. If the pressure decreases from zero to −13 cmH_2O in 2 s (part or all of a normal inspiratory time), the vibration frequency is ~30/s. Therefore, this model-predicted uvula/tongue vibration is similar to real snoring.

DISCUSSION

In this study, we develop a pressure- and state-dependent muscle contraction model that can mimic genioglossal muscle activation behaviors and can be conveniently incorporated into a finite element model of the upper airway. The advantage of this model is that it builds a bridge between the contractile force and the measured EMG signals. Therefore, one can directly incorporate the measured EMG data and effectively avoid the difficulty in determining muscle shortening velocity during complex pharyngeal conditions when modeling the muscle's contractile behaviors. This makes it possible to input an individual's anatomical structure (magnetic resonance imaging), muscle activation information (EMG), and standard tissue mechanical properties into the computational model and produce a detailed finite element analysis of upper airway collapsibility. This muscle contraction model, developed on the basis of experimental observations, is very applicable and can correctly mimic the contractile behaviors of genioglossal muscle. Of course, as more experimental data on the structure, mechanical property, and activity pattern of the genioglossal muscle evolve, this contraction model can also be adjusted to allow the incorporation of new information.

As shown in Table 2, the stretch of muscle fiber under given negative pressures is sensitive to the parameter m, which quantifies the nonlinear nature of the relationship between the total number of cross bridges and A_{EMG} (Eq. 4 would be linear if $m = 1$). Our results show that m should be much larger than 1; therefore, the relationship between the number of cross bridges and A_{EMG} is very nonlinear. Without direct experimental data, it is hard to estimate the error produced by using the measured EMG to predict the number of cross bridges. However, currently available experimental results on the relationship between EMG and tension suggest that our model can predict muscle behaviors similar to that observed in isometric muscle experiments (5). In our simulation, two major variables can contribute to the contractile force: one is the total number of the attached cross bridges, and the other is the displacement of the cross bridges (see Eqs. 4 and 5). Varying either of them can change the contractile force. The model predicts that, during waking, the length of the activated genioglossal muscle fiber, whose cross-bridge number is predicted using the EMG, is maintained in a large range of negative pressures (see Fig. 5), and, therefore, the muscle is roughly isometric. From Fig. 4, we can see that, in the same pressure range, the relationship

between EMG and stress is quite linear. This is consistent with the observed relationship between EMG and tension in isometric muscle experiments (5).

An important variable that affects the contractile ability of skeletal muscle is the length of the sarcomere. The developed tension is directly related to the degree of overlap between myosin and actin filaments in individual sarcomeres (25, 26, 44). The isometric length-tension experiment performed by Gordon et al. (16) shows that the developed tension is a nonlinear function of the sarcomere length, with the greatest developed tension found near the length it occupies in the body. There is a plateau in the developed tension when the sarcomere length is in the range of 2.0–2.25 μm (a 12.5% stretch). In our muscle contraction model, we did not model the effect of the muscle fiber length on the number of cross bridges and, therefore, on the contractile force. This was due to the following consideration. Using the −5-cmH_2O P_{close} of the normal male passive airway and the Young's modulus of the passive tongue E = 6,000 Pa, one can estimate that the maximum muscle stretch ($-P_{close}/E$) reached when the upper airway is fully collapsed is only ~8%. For apnea patients, the maximum stretch is even smaller due to a narrower upper airway and sometimes a bigger tongue in these patients. Therefore, there is little effect of the length of genioglossal muscle fibers on the number of cross bridges during upper airway collapse.

When modeling the parallel element, we assumed that connective tissue can be described as linear elastic material. Generally, the elastic behavior of a passive muscle is not simply linear (14, 44). A muscle can get stiffer when it is extended. Therefore, the tension curve for a passive muscle gets steeper at larger stretch. However, as described above, the maximum stretch of the genioglossal muscle during upper airway collapse is <8%. In this displacement range, a linear elastic material assumption for the passive tongue seems acceptable.

The soft palate and uvula consist of different muscles, such as the levator veli palatini, tensor veli palatini, palatoglossus, palatopharyngeus, and muscular uvula, which show different contractile behaviors. The palatoglossus has prominent inspiratory phasic activation, but the tensor palatini has no such phasic activation, whereas the levator platini varies between inspiratory and expiratory activation (45, 56, 57). These muscle fiber orientations are much more complex than that of genioglossal muscle, and many of them, such as the orientation of the palatopharyngeus, are mainly in the lateral direction. Thus it is impractical to directly simulate the activation of the soft palate and uvula muscles in such a two-dimensional approximation of the pharyngeal airway. Our major objective in this study was to develop and test the contraction model for the genioglossal muscle and simulate tongue movement under negative upper airway pressure conditions. Therefore, in the present two-dimensional upper airway simulation, instead of directly mimicking the soft palate and uvula muscle activity, we simply described them as elastic materials. In addition, we introduced a "moving-together" assumption and accounted for the effects of the muscle contraction of the soft palate and uvula under different pharyngeal states (passive, sleep, and wake) by giving a different elastic modulus. Under such an approximation, the uvula can move together with the tongue during a decrease in airway pressure but not result in a significant resistance to tongue movement. This is an approximation for the current two-dimensional simulation of upper airway collapse but likely approximates the actual situation. A realistic simulation of the contraction of the soft palate muscles would necessitate upper airway tissue deformation in the lateral direction, which is not possible with a two-dimensional model. In the future, we plan to develop a muscle contraction model for the soft palate and uvula using methods similar to those for the genioglossal muscle model and apply it to a three-dimensional simulation of human upper airway deformation.

To test our contraction model of genioglossal muscle, we incorporated it into our two-dimensional finite element model of the human pharyngeal airway. Although this is a two-

dimensional model, it maintains the major features of tongue and uvula movement in the anterioposterior direction (7, 21). A number of mathematical models have been developed to describe upper airway behaviors in recent years. However, because the human pharyngeal airway is a very complex mechanical system involving irregular geometric structures and tissues with different mechanical properties and functions (including muscle contraction), it is not an easy task to model the flow, deformation, and collapse of the human upper airway. Thus extensive simplifications have been utilized in these models. The collapsible tube models are used to describe flow, pressure-volume, or pressure-cross-sectional area relationships, or to help interpret the experimental findings of collapse and obstruction in the upper airway. Aittokallio et al. (1) recently developed a new collapsible tube model to simulate the snorer's upper airway. Using the model, Aittokallio et al. analyzed the flow and cross-sectional area changes of the tube and predicted nasal flow profile. In addition, using a modified model involving upper airway forces, they also predicted the inspiratory flow shapes during sleep (2). However, collapsible tube models are far from realistic simulations of the collapse in the upper airway. The human pharynx is far from an axisymmetric tube not only in its geometric structure but also in the mechanical properties and functions of its surrounding tissues. To investigate upper airway collapse, Gavriely and Jensen (15) modeled the human upper airway by a movable segment supported by a spring that is connected to a rigid channel having a rectangular cross section and resistance to flow. Using this lumped-parameter model, they investigated the effects of geometric parameters, resistance, compliance, and gas density on upper airway closure. Their model predicted that the width and length of the movable portion of the upper airway and the gas density are likely to affect the onset of snoring (15). Huang and Williams (23) developed another lumped-parameter model, which simulated the deformation of the upper airway wall by a piston having damping and elastic functions, to analyze the neuromechanical interaction in human snoring and upper airway obstruction and demonstrated the importance of delay in the muscle reflex to airway negative pressure during sleep. Using an orifice flow model, Leiter (36) investigated the relationships among pressure, flow, orifice shape and orientation, and genioglossal EMG in the human pharyngeal airway during inspiration, which suggested that genioglossal muscle shortening increased pharyngeal area and reduced pharyngeal resistance more effectively when the pharynx is elliptical, with the long axis of the ellipse oriented laterally. Different mechanical models developed in past years have contributed greatly to our understanding of upper airway physiological processes. However, all the above models importantly simplify the upper airway geometric structures and muscle mechanical properties, and such lumped-parameter models cannot provide localized details of upper airway flow and deformation.

Shome et al. (53) developed a three-dimensional model of airflow in the human pharynx to investigate the effect of turbulence and flow rate on airflow characteristics. Although they used anatomically correct geometric structures, this model cannot be used to simulate tissue deformation and upper airway collapse because it is a pure flow model in a rigid upper airway. The major differences between our upper airway model and the above models are the following. First, our construction of the upper airway geometry is based on the realistic anatomical structure of the midsagittal plane of the human upper airway, and therefore our model is anatomically correct. Second, our model simulates both air flow and tongue movement, which involves strong air-tissue interactions on the deformable interfaces of air-uvula, air-tongue, and air-epiglottis. Third, this is not a lumped-parameter model but a detailed simulation of flow and tissue status, including local deformation and movement of the tongue under outside load and muscle contraction.

The feasibility of using such a two-dimensional model to simulate air flow and tissue deformation and investigate upper airway collapsibility has been demonstrated in our earlier simulation of the passive upper airway (22, 37). Two results strongly support the validity of

such a two-dimensional approximation. First, by matching the measured −5-cmH_2O P_{close} in the male passive airway (27), we predicted a 6,000-Pa Young's modulus of the passive tongue using our two-dimensional model, which is almost identical to the value 6,200 Pa, the measured Young's modulus of passive skeletal muscle (8, 34). Second, using our passive male airway model with the same tissue mechanical properties but different anatomies for a female model, we predicted that −7-cmH_2O pressure would be required to collapse the female passive airway. This is again similar to Isono [2 female studies (personal communication)]. Therefore, this two-dimensional approximation of the upper airway seems to accurately describe the pharyngeal muscle behaviors during the process of airway collapse.

In the presented study, a laminar model was used for the flow simulation. This laminar flow approximation has potential limitations because it cannot apply to all types of flow regimes that can exist in the pharyngeal airway. During upper airway collapse, with the pressure decreasing gradually from 0 cmH_2O to the P_{close}, the flow in a normal upper airway will progress from laminar to nonlaminar (which is mainly a transition from laminar to turbulent flow), and then to laminar flow again when the flow rate decreases substantially (low Reynolds number) before the upper airway is fully collapsed. If a laminar flow model is used to predict the airway pressure (not the P_{close}) for a specific situation, such as 30 or 50% airway collapse (not full collapse), it will produce inaccurate results if the Reynolds number is high. However, our primary purpose is to predict the upper airway P_{close}. As stated above, the flow before pharyngeal obstruction should be laminar. Therefore, we believe this laminar flow model serves our purpose well.

Upper airway collapse is fundamentally a complex three-dimensional problem. The muscle behaviors are also very complex. As mentioned in the introduction, we realize that, in addition to the genioglossus muscle, other intrinsic and extrinsic tongue muscles, additional pharyngeal dilator muscles, as well as pharyngeal constrictor muscles are also active during respiration and contribute to upper airway patency. Therefore, limitations exist in our model if one is looking for a complete clinical prediction of upper airway collapse, because we do not incorporate the full effects of activation of these additional muscles. Currently, there are no available data addressing the activity of either other extrinsic or intrinsic tongue muscles during sleep in humans. A rat study performed by Fuller et al. (12) suggests that progressive increases in respiratory drive are associated with the coactivation of the tongue protrudor (genioglossus) and retractor (styloglossus and hyoglossus) muscles and that this coactivation causes retraction of the tongue. In addition, a human study performed by Mateika et al. (41) demonstrated a coactivation of the tongue protrudor and retractor muscles during hypercapnia and asphyxia while awake. On the other hand, in a human study of five apnea patients (9), it was demonstrated that coactivation of the tongue protrudor and retractor muscles, if it really occurs in humans during normal breathing, yielded an ~10% difference in maximal airway flow from genioglossus activation alone. Finally, a human study performed by Kobayashi et al. (32) reported that, during rapid inspiration, the posterior edge of the tongue moved forward (not backward), which suggests that the genioglossus muscle may dominates the tongue's contractile behaviors during inspiration. In the pharyngeal constrictor muscle studies, Kuna (35) examined the respiratory-related activation of these muscles in decerebrate cats, normal adult humans, and patients with obstructive sleep apnea. The results showed that selective activation of the constrictor muscles could stiffen the pharyngeal airway and could constrict the airway at relatively high airway volume but dilate the airway at relatively low airway volume (35). Thus we need to emphasize that, although we only directly modeled genioglossal muscle contraction in the present study, we do not claim that the genioglossus is the only active tongue muscle during wakefulness or sleep. Because our major purpose in simulating upper airway deformation in this paper was to test our genioglossal muscle contraction model and to determine how the activation of this

specific muscle influenced the tongue deformation during wakefulness and sleep, we did not directly simulate other tongue muscle activity in this two-dimensional simulation of the upper airway collapse. Thus we did not model the complete clinical scenario. We would like to indicate, however, that in our simulation of the upper airway collapse, the overall effect of other upper airway muscles is, in fact, partly reflected in the parameters c and m in Eq. 5. We determined these parameters assuming constant airway area during wakefulness, which results from the contributions of all pharyngeal muscles. For a more accurate simulation of upper airway flow, deformation, and collapse under different conditions and a deeper investigation into the pathophysiology of obstructive sleep apnea, we must and have begun to develop a more realistic computational model based on the three-dimensional anatomical structure of the human upper airway. Additional pharyngeal muscles and their behaviors will be simulated in the new model. We believe that such a three-dimensional computational model, including simulations of pharyngeal anatomy, muscle activity, and tissue mechanical properties, can play an important role in future studies of pharyngeal pathophysiology, surgical planning, and the development of new therapies for obstructive sleep apnea.

Acknowledgments

GRANTS

This research was supported by National Heart, Lung, and Blood Institute Grants 1 P50 HL-60292 and RO1 HL-48531, the Sleep Medicine and Education Research Foundation of the American Academy of Sleep Medicine, and the American Heart Association.

References

1. Aittokallio T, Gyllenberg M, Polo O. A model of a snorer’s upper airway. Math Biosci. 2001; 170:79–90. [PubMed: 11259804]
2. Aittokallio T, Gyllenberg M, Saaresranta T, Polo O. Prediction of inspiratory flow shapes during sleep with a mathematical model of upper airway forces. Sleep. 2003; 26:857–863. [PubMed: 14655920]
3. Akahoshi T, White DP, Edwards JK, Beauregard J, Shea SA. Phasic mechanoreceptor stimuli can induce phasic activation of upper airway muscles in humans. J Physiol. 2001; 531:677–691. [PubMed: 11251050]
4. Ayas N, Malhotra A, Epstein L. Alternative therapies for sleep apnea. Drugs Today. 1999; 35:811–821. [PubMed: 12973373]
5. Basmajian, JV. Muscles Alive. Baltimore, MD: Williams & Wilkins; 1978.
6. Bathe, KJ. Finite Element Procedures. Englewood Cliffs, NJ: Prentice Hall; 1996.
7. Ciscar MA, Juan G, Martinez V, Ramon M, Lloret T, Minguez J, Armengot M, Marin J, Basterra J. Magnetic resonance imaging of the pharynx in OSA patients and healthy subjects. Eur Respir J. 2001; 17:79– 86. [PubMed: 11307760]
8. Duck, F. Physical Properties of Tissue: a Comprehensive Reference Book. London: Academic; 1990.
9. Eisele DW, Smith PL, Alam DS, Schwartz AR. Direct hypoglossal nerve stimulation in obstructive sleep apnea. Arch Otolaryngol Head Neck Surg. 1997; 123:57–61. [PubMed: 9006504]
10. Fogel RB, Trinder J, Malhotra A, Stanchina M, Edwards JK, Schory KE, White DP. Within-breath control of genioglossal muscle activation in humans: effect of sleep-wake state. J Physiol. 2003; 550:899–910. [PubMed: 12807995]
11. Fogel RB, White DP, Pierce RJ, Malhotra A, Edwards JK, Dunai J, Kleverlaan D, Trinder J. Control of upper airway muscle activity in younger versus older men during sleep onset. J Physiol. 2003; 553:533–544. [PubMed: 12963804]
12. Fuller D, Mateika JH, Fregosi RF. Co-activation of tongue protrudor and retractor muscles during chemoreceptor stimulation in the rat. J Physiol. 1997; 507:265–276. [PubMed: 9490849]
13. Fung, YC. Biomechanics: Motion, Flow, Stress, and Growth. New York: Springer-Verlag; 1990.

14. Fung, YC. Biomechanics: Mechanical Properties of Living Tissue. New York: Springer-Verlag; 1993.
15. Gavriely N, Jensen O. Theory and measurements of snores. J Appl Physiol. 1993; 74:2828–2837. [PubMed: 8365987]
16. Gordon AM, Huxley AF, Julian FJ. The variation in isometric tension with sarcomere length in vertebrate muscle fiber. J Physiol. 1966; 185:170–192. [PubMed: 5921536]
17. Hashimoto K, Suga S. Estimation of muscular tension of the human tongue by using a three-dimensional model of the tongue. J Acoust Soc Jpn. 1986; 7:39– 46.
18. Horner RL, Innes JA, Holden HB, Guz A. Afferent pathway(s) for pharyngeal dilator reflex to negative pressure in man: a study using upper airway anaesthesia. J Physiol. 1991; 436:31–44. [PubMed: 2061834]
19. Horner R, Innes J, Morrell M, Shea S, Guz A. The effect of sleep on reflex genioglossus muscle activation by stimuli of negative airway pressure in humans. J Physiol. 1994; 476:141–151. [PubMed: 8046629]
20. Horner RL, Innes JA, Murphy K, Guz A. Evidence for reflex upper airway dilator muscle activation by sudden negative airway pressure in man. J Physiol. 1991; 436:15–29. [PubMed: 2061830]
21. Horner RL, Shea SA, McIvor J, Guz A. Pharyngeal size and shape during wakefulness and sleep in patients with obstructive sleep apnoea. QJM. 1989; 72:719–735. [PubMed: 2602554]
22. Huang Y, Malhotra A, Fogel R, Pillar G, Kikinis R, Loring S, White DP. A finite element analysis of gender differences in upper airway structure (Abstract). Am J Respir Crit Care Med. 2001; 163:A635.
23. Huang L, Williams JE. Neuromechanical interaction in human snoring and upper airway obstruction. J Appl Physiol. 1999; 86:1759–1763. [PubMed: 10368334]
24. Hung J, Whitford EG, Parsons RW, Hillman DR. Association of sleep apnoea with myocardial infarction in men. Lancet. 1990; 336:261–264. [PubMed: 1973968]
25. Huxley AF. Muscle structure and theories of contraction. Prog Biophys Biophys Chem. 1957; 7:255–318. [PubMed: 13485191]
26. Huxley AF, Simmons RM. Proposed mechanism of force generation in striated muscle. Nature. 1971; 233:533–538. [PubMed: 4939977]
27. Isono S, Remmers JE, Tanaka A, Sho Y, Sato J, Nishino T. Anatomy of pharynx in patients with obstructive sleep apnea and in normal subjects. J Appl Physiol. 1997; 82:1319–1326. [PubMed: 9104871]
28. Jenkinson C, Stradling J, Petersen S. Comparison of three measures of quality of life outcome in the evaluation of continuous positive airways pressure therapy for sleep apnoea. J Sleep Res. 1997; 6:199–204. [PubMed: 9358398]
29. Jenkinson C, Davies RJ, Mullins R, Stradling JR. Comparison of therapeutic and subtherapeutic nasal continuous positive airway pressure for obstructive sleep apnoea: a randomised prospective parallel trial. Lancet. 1999; 353:2100–2105. [PubMed: 10382693]
30. Johansson T, Meier P, Blickhan R. A finite-element model for the mechanical analysis of skeletal muscle. J Theor Biol. 2000; 206:131–149. [PubMed: 10968943]
31. Kier MK, Smith KK. Tongue tentacles and trunks: the biomechanics of movement in muscular-hydrostats. Zoolog J Linnean Soc. 1985; 83:307–324.
32. Kobayashi I, Perry A, Rhymer J, Wuyam B, Hughes P, Murphy K, Innnes JA, McIvor J, Cheesman AD, Guz A. Inspiratory coactivation of the genioglussus enlarges retroglossal space in laryngectomized humans. J Appl Physiol. 1996; 80:1595–1604. [PubMed: 8727545]
33. Kojic M, Mijailovic S, Zdravkovic N. Modeling of muscle behavior by the finite element method using Hill's three-element model. Int J Numer Meth Eng. 1998; 43:941–953.
34. Krouskop TA, Dougherty DR, Vinson FS. A pulsed doppler ultrasonic system for making noninvasive measurements of the mechanical properties of soft tissues. J Rehabil Res Dev. 1987; 24:1–8. [PubMed: 3295197]
35. Kuna ST. Respiratory-related activation, and mechanical effects of the pharyngeal constrictor muscles. Respir Physiol. 2000; 119:155–161. [PubMed: 10722858]

36. Leiter JC. Analysis of pharyngeal resistance and genioglossal EMG activity using a model of orifice flow. J Appl Physiol. 1992; 73:576–583. [PubMed: 1399983]
37. Malhotra A, Huang Y, Fogel R, Pillar G, Edwards JK, Kikinis R, Loring SH, White DP. The male predisposition to pharyngeal collapse: importance of airway length. Am J Respir Crit Care Med. 2002; 166:1388–1395. [PubMed: 12421747]
38. Malhotra A, Pillar G, Fogel RB, Edwards JK, Ayas N, Akahoshi T, Hess D, White DP. Pharyngeal pressure and flow effects on genioglossus activation in normal subjects. Am J Respir Crit Care Med. 2002; 165:71–77. [PubMed: 11779733]
39. Malhotra A, Pillar G, Fogel RB, Edwards JK, Beauregard J, White DP. Upper airway collapsibility: measurement and sleep effects. Chest. 2001; 120:156–161. [PubMed: 11451832]
40. Malhotra A, White D. Seminar: obstructive sleep apnoea. Lancet. 2002; 360:237–245. [PubMed: 12133673]
41. Mateika JH, Millrood DL, Kim J, Rodriguez HP, Samara GJ. Response of human tongue protrudor and retractors to hypoxia and hypercapnia. Am J Respir Crit Care Med. 1999; 160:1976–1982. [PubMed: 10588616]
42. Mathew OP, Abu-Osba YK, Thach BT. Influence of upper airway pressure changes on genioglossus and muscle respiratory activity. J Appl Physiol. 1982; 52:438– 444. [PubMed: 7037716]
43. Mathew OP, Abu-Osba YK, Thach BT. Genioglossus muscle response to upper airway pressure changes: afferent pathways. J Appl Physiol. 1982; 52:445–450. [PubMed: 7061298]
44. McMahon, TA. Muscles, Reflexes, and Locomotion. Princeton, NJ: Princeton Univ. Press; 1984.
45. Mezzanotte WS, Tangel DJ, White DP. Influence of sleep onset on upper-airway muscle activity in apnea patients versus normal controls. Am J Respir Crit Care Med. 1996; 153:1880–1887. [PubMed: 8665050]
46. Nadapow V. A biomechanical model of sagittal tongue bending. J Biomech Eng. 2002; 124:547–556. [PubMed: 12405598]
47. Parmly WW, Sonnenblick EH. Series elasticity in heart muscle. Circ Res. 1967; 20:112–123. [PubMed: 6017705]
48. Peppard P, Young T, Palta M, Skatrud J. Prospective study of the association between sleep disordered breathing and hypertension. N Engl J Med. 2000; 342:1378–1384. [PubMed: 10805822]
49. Sanguineti V. A control model of human tongue movements in speech. Biol Cybern. 1997; 77:11–22. [PubMed: 9309860]
50. Schwartz AR, Smith PL, Wise RA, Gold AR, Permutt S. Induction of upper airway occlusion in sleeping individuals with subatmospheric nasal pressure. J Appl Physiol. 1988; 64:535–542. [PubMed: 3372411]
51. Shahar E, Whitney CW, Redline S, Lee ET, Newman AB, Nieto FJ, O'Connor GT, Boland L, Schwartz JE, Samet JM. Sleep-disordered breathing and cardiovascular disease: cross-sectional results of the Sleep Heart Health Study. Am J Respir Crit Care Med. 2001; 163:19–25. [PubMed: 11208620]
52. Shea SA, Edwards JK, White DP. Effect of wake-sleep transitions and rapid eye movement sleep on pharyngeal muscle response to negative pressure in humans. J Physiol. 1999; 520:897–908. [PubMed: 10545152]
53. Shome B, Wang LP, Santare MH, Prasad AK, Szeri AZ, Roberts D. Modeling of airflow in the pharynx with application to sleep apnea. J Biomech Eng. 1998; 120:416– 422. [PubMed: 10412410]
54. Smith KK, Kier MK. Trunks, tongues, and tentacles: moving with skeletons of muscle. Am Sci. 1989; 77:29–35.
55. Stanchina M, Malhotra A, Fogel RB, Ayas NT, Edwards JK, Schory K, White DP. Genioglossus muscle responsiveness to chemical and mechanical loading during NREM sleep. Am J Respir Crit Care Med. 2002; 165:945–949. [PubMed: 11934719]
56. Tangel DJ, Mezzanotte WS, Sandberg EJ, White DP. The influence of NREM sleep on the activity of tonic postural vs. inspiratory phasic muscles in normal men. J Appl Physiol. 1992; 73:1058–1066. [PubMed: 1400018]

57. Tangel DJ, Mezzanotte WS, White DP. Respiratory-related control of palatoglossus and levator palatini muscle activity. J Appl Physiol. 1995; 78:680– 688. [PubMed: 7759440]
58. Van Lunteran E, Strohl KP. The muscles of the upper airways. Clin Chest Med. 1986; 7:171–188. [PubMed: 3522067]
59. Worsnop C, Kay A, Pierce R, Kim Y, Trinder J. Activity of respiratory pump and upper airway muscles during sleep onset. J Appl Physiol. 1998; 85:908–920. [PubMed: 9729564]
60. Yamada, H. Strength of Biological Materials. Baltimore, MD: Williams and Wilkins; 1970.
61. Young T, Palta M, Dempsey J, Skatrud J, Weber S, Badr S. The occurrence of sleep-disordered breathing among middle-aged adults. N Engl J Med. 1993; 32:1230–1235. [PubMed: 8464434]

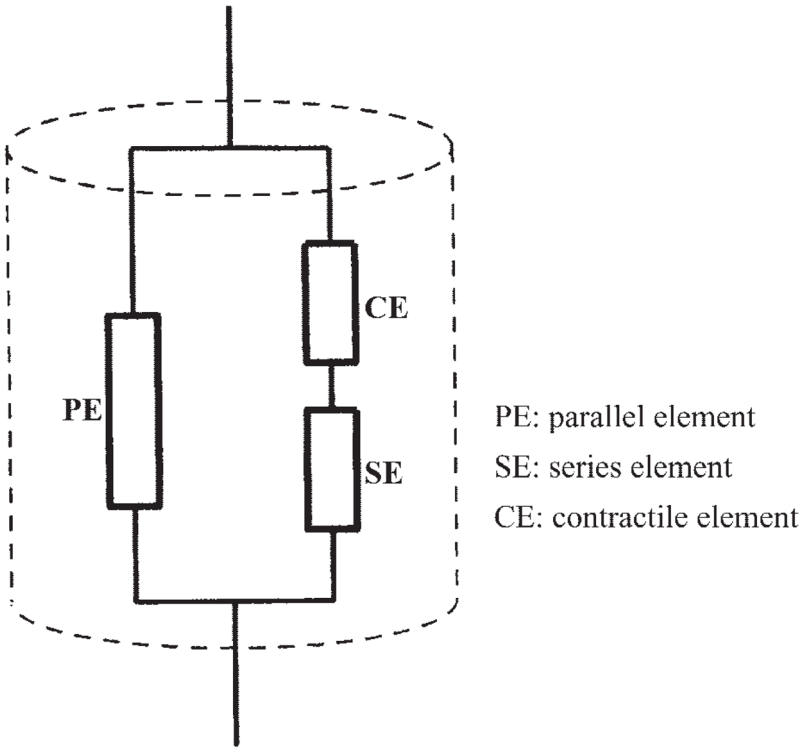

Fig. 1.
Three-element contraction model of the genioglossal muscle.

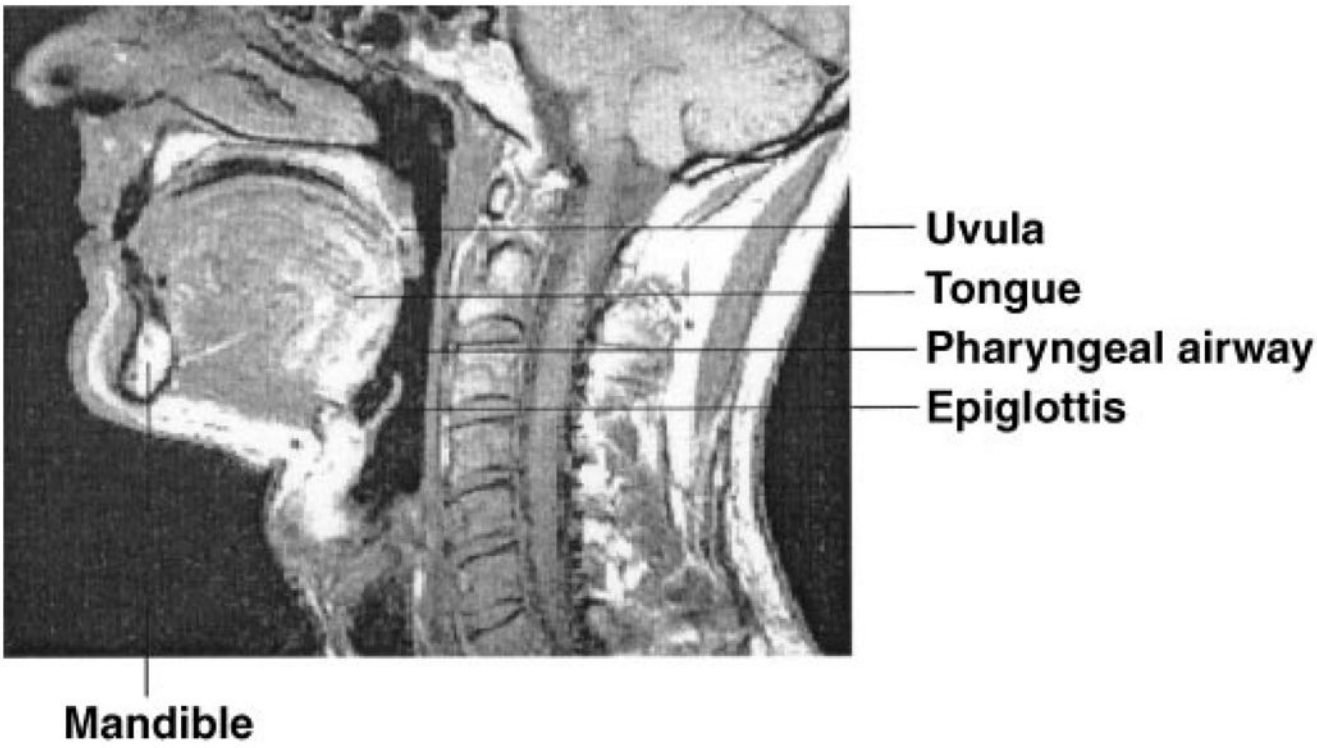

Fig. 2.
Midsagittal plane magnetic resonance image showing the typical structure of the pharyngeal airway in a normal subject.

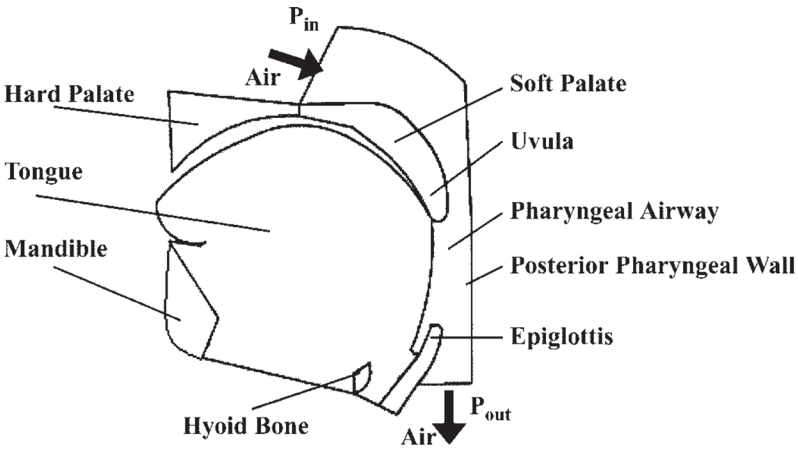

Fig. 3.

Representative mean structure of the male upper airway derived from 5 randomly selected magnetic resonance images of normal men. P_{in}, pressure at the inlet to the upper airway; P_{out}, pressure at the outlet.

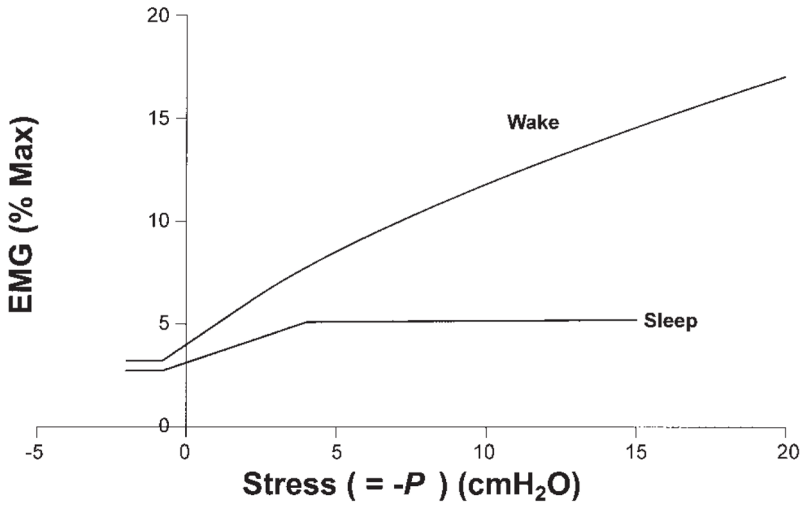

Fig. 4.

Electromyogram (EMG) amplitude vs. normal stress (=−P) curves used to test our contraction model. Data for the waking condition are obtained from published results (3). For the sleeping airway, we estimated that both tonic and phasic genioglossal muscle activities decrease by ~15% during normal breathing (P ≥ peak negative pressure) based on the literature and that phasic activation increases slowly when upper airway pressure becomes more negative due to a substantial reduction but not complete loss of reflex mechanisms. EMG activities before 0 stress (while airway pressure is positive) are preactivation likely resulting from phasic respiratory input.

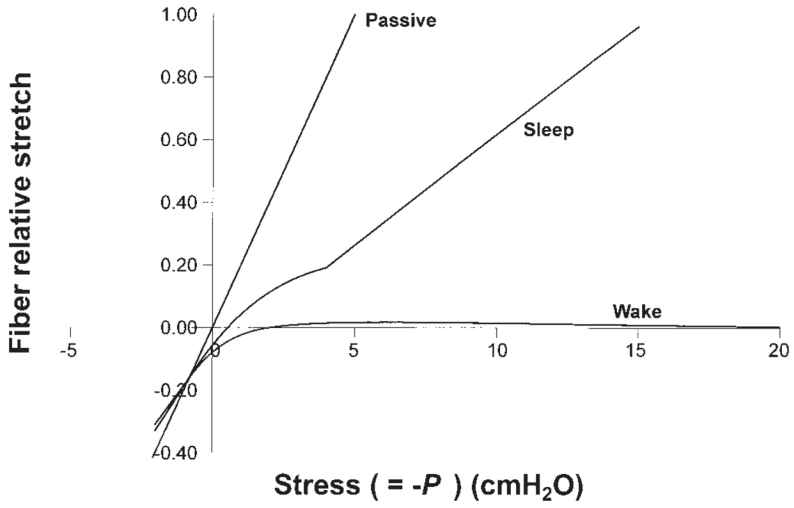

Fig. 5.

Predicted stretch of the genioglossal muscle fiber during different upper airway pressures and states (passive, sleep, and wake), which is normalized by the stretch of the passive muscle fiber at −5 cmH_2O. Curves for sleep and wake are obtained based on the EMG-pressure curves in Fig. 4 for sleep and wake, respectively.

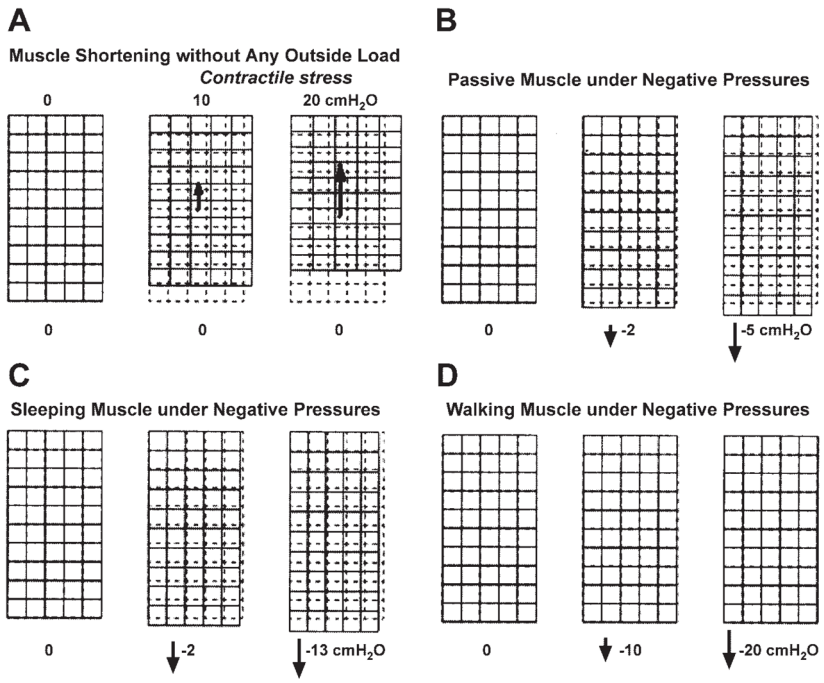

Fig. 6.

Simulations of the genioglossal muscle under different conditions. Each large rectangle represents the genioglossal muscle with a vertical fiber orientation. The *top left* of each muscle is fixed. The remainder of the upper boundary can only move horizontally, and the lower boundary is fully free. *A*: muscle shortens with the increase of the contractile stress without any outside load. *B*–*D*: negative pressures are loaded on the lower boundary of the muscle, and the muscle deforms under passive (*B*), sleeping (*C*), and waking (*D*) conditions.

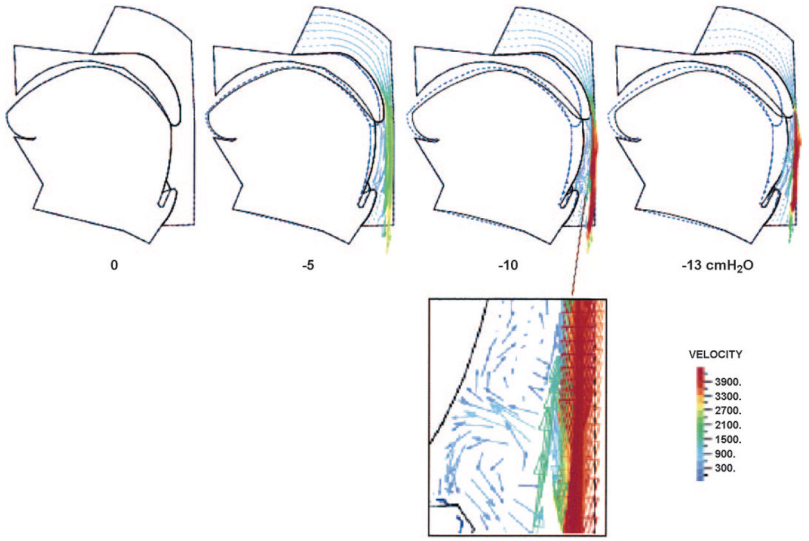

Fig. 7.

Air flow and collapse of sleeping upper airway under negative pressures. Dashed lines give the initial locations of the tongue and uvula at zero pressure, and the solid lines show their positions at the given airway negative pressure. See text for further discussion.

Table 1

Input parameters

Parameter	Value	Ref. No.
E (tongue, passive)	6,000 Pa	8, 34
L_{sar}	2.1 μm	14, 44
ν^*	0.49	
$\alpha^\dagger$	0.4/% muscle length	47
$\beta^\dagger$	0.4 g/% muscle length	47
E (hard palate, hyoid bone)	1.72×10^{10} Pa	60
E (epiglottis)	1.63×10^{6} Pa	60
ρ	0.0012 g/cm^3	13
μ	1.8×10^{-4} P	14
P_{peak} (inspiration, wake)	−2 cmH_2O	3
P_{peak} (inspiration, sleep)	−4 cmH_2O	our data
$y_0^\ddagger$	13.7 nm	
$c^\ddagger$	1.41×10^{7} Pa	
$m^\ddagger$	2.3	

E, elastic modulus; L_{sar}, length of sarcomere; V, Poission ratio of a given elastic material; α and β, constants in series element model; ρ, density of air; μ, viscosity of air; P_{peak}, peak epiglottes pressure; y_0, required displacement for generating contractile force; c, parameter in muscle contraction model (see Eq. 5); m, constant in cross-bridge model (see Eq. 4).

*Based on an assumption that the tongue is almost incompressible.

†These values are for heart muscle, and their definitions are somewhat different from ours. They will be transformed to the values under our definition. Also, to account for the difference in the extension shown in isotonic quick-release experiments between skeletal and heart muscle, we use a β value twice the one utilized for heart muscle.

‡See *Parameter determination* and *Model inputs*.

Table 2

Sensitivity analysis of parameters

		Effects on Relative Change in Fiber Length, $\Delta L/\Delta L_0$, %							
		Sleep: P, cmH_2O				Wake: P, cmH_2O			
Parameter	**Variation, %**	**−2**	**−4**	**−10**	**−13**	**−2**	**−5**	**−13**	**−20**
Baseline		13.6	23.2	74.9	100.0	−0.04	2.05	1.32	0.41
E	−30	15.9	26.1	83.9	112.0	−0.05	2.15	1.35	0.41
	30	11.9	20.9	67.6	90.3	−0.02	1.95	1.30	0.40
α	−30	13.7	23.3	75.1	100.0	−0.04	2.28	1.95	1.42
	30	13.6	23.2	74.7	99.9	−0.10	1.92	0.98	−0.15
β	−30	13.6	23.3	75.1	100.3	−0.04	2.27	1.97	1.40
	30	13.6	23.2	74.7	99.8	−0.07	1.92	0.98	−0.13
A_{EMG}	−30	26.9	46.5	127.2	166.8	12.7	21.0	22.6	20.7
	30	3.81	8.67	42.6	59.0	−7.16	−6.55	−7.01	−7.25
c	−30	19.6	33.1	97.1	128.4	5.16	9.15	8.84	7.45
	30	9.22	16.5	59.8	80.9	−3.41	−2.17	−2.85	−3.43
m	−30	29.1	54.9	146.7	192.2	19.7	41.9	71.3	84.0
	30	−1.43	−0.73	21.44	32.0	−12.2	−13.3	−14.4	−14.3
y_0	−30	16.6	26.9	78.6	103.8	4.12	6.98	6.79	6.01
	30	10.6	19.5	71.1	96.3	−4.19	−2.89	−4.14	−5.18

ΔL and ΔL_0 are the change in the muscle fiber length for the modified parameters and the reference parameters, respectively. A_{EMG}, EMG amplitude.